JOURNAL OF MATERIALS SCIENCE 19 (1984) 1359–1373

The fracture process of ultra-high strength polyethylene fibres

JAN SMOOK, WIM HAMERSMA, ALBERT J. PENNINGS
Laboratory of Polymer Chemistry, State University of Groningen, Nijenborgh 16, 9747 AG Groningen, The Netherlands

The fracture behaviour of ultra-high strength polyethylene fibres has been investigated in dead load tests as well as by electron microscopical observation of the fracture surfaces. It was found that the fracture process in the fibres involves an activation energy of about 60 to 75 kJ mol^{-1}, which implies that the strength is mainly determined by the lateral bond strength between the molecules. Fracture is initiated at surface irregularities, such as kink bands, which leads to the formation of cracks with a fibrillated fracture surface. In this process the individual fibrils are cut through at topological defect regions in such fibrils, containing a relatively high concentration of trapped entanglements and chain ends. The ultimate strength of the polyethylene fibres was found to be inversely proportional to the square root of its diameter. Extrapolation to zero diameter yields a strength of 26 GPa for flawless fibres, which equals the theoretical strength of polyethylene.

1. Introduction

The development of new, strong polymeric materials has attracted a good deal of interest during the last two decades, because the combination of a high potential strength and a low density makes such materials desirable for many applications. The extensive activity in this field resulted in new, strong fibre materials, such as poly(*p*-phenylene)terephtalamide [1, 2], carbon fibres [3] and ultra-high strength polyethylene fibres [4–8]. For the preparation of the ultra-high strength polyethylene fibres, two methods are available in our laboratory, i.e. the so-called "surface growth" method [4, 5] and the technique of gel-spinning and hot-drawing [6–8]. The essential feature in both techniques is the transformation of a dilute entanglement network in solutions of ultra-high molecular weight polyethylene (UHMWPE) into highly oriented crystalline structures. This allows the formation of fibres with a tensile strength at fracture up to 5 GPa. Although the strength level of such UHMWPE fibres is unusually high, it is still far from the intrinsic strength of the C–C bond in polyethylene, which is estimated to be about 25 GPa [9–11]. A further development of the intrinsic strength properties of the UHMWPE, if possible at all, has however been hampered by a limited understanding, at present, of the complex fracture mechanics in polymers.

Therefore it was the purpose of this study to investigate the fracture mechanism of the highly oriented UHMWPE fibres under various conditions. The lifetimes of the UHMWPE fibres have been measured in dead-load tests at various temperatures and some morphological features of the fracture surfaces have been observed.

It will be shown that at temperatures below 100° C the fracture in the UHMWPE fibres involves an activation energy of about 60 to 75 kJ mol^{-1}, implying that fracture is a combined process of chain scissioning and the breakage of lateral bonds between the polymer molecules. At higher temperatures creep failure will dominate more and more. Electron microscopical investigations have revealed that fracture is initiated from surface irregularities, such as kink bands, leading to crack formation with a fibrillated fracture surface. It has also been observed that the ultimate strength of the UHMWPE fibres depends on the fibre diameter,

0022–2461/84 $03.00 + .12

analogous to the early observations of Griffith [9] on glass fibres.

2. General background to polymer fracture

It is well known that all preparation techniques of oriented polymeric fibres lead to practical strengths which are considerably lower than the theoretical maximum strength. This theoretical maximum strength is to be achieved in an array of fully aligned and elongated chain-molecules of infinite length. The strength would then be determined by the weakest bond in the polymer chain, i.e. the C–C bond in polyethylene.

An estimate of the theoretical strength may be obtained from the potential energy function describing the interatomic forces as a function of the atomic separation. However, the values, thus obtained for the theoretical strength in polyethylene, are quite dependent on the approximation of the potential energy function used in the calculations. With a simple Morse potential function a value of about 25 GPa [10–12] is obtained for the ultimate strength in polyethylene. More recent calculations, using Hartree–Fock self consistent field methods yield quite different values, i.e. Boudreaux [13] estimated a value of 19 GPa and Crist *et al.* [14] obtained 66 GPa for the maximum strength in polyethylene at 0 K.

Although the Morse potential function is undoubtedly oversimplified, it still seems to give the most trustworthy result at present, since the Hartree–Fock approximation especially leads to large deviations in the interaction energy between the atoms at large atomic separations [15]. Moreover the "Morse" value of 25 GPa coincides very well with a general rule of thumb, that the ultimate strength is about 1/10 of the modulus. The theoretical modulus in polyethylene is calculated somewhere between 250 and 350 GPa.

In practice, the strength of materials is limited by the presence of flaws, cracks and imperfections. Griffith [9] introduced the idea that fracture is initiated at flaws, which leads to the formation of a crack. Once a crack reaches a critical dimension, the solid will fail in a dramatic way. According to Griffith a necessary condition for the formation of a crack of critical dimensions is that the strain energy stored in the medium is equal or greater than the energy required to create new surfaces, which yields for the strength

$$\sigma = (2\gamma E/\pi c)^{1/2} \qquad (1)$$

where σ is tensile strength, E is Young's modulus, γ is surface energy and c is the length of the crack. This expression is, however, only valid for the formation of a crack in an infinite plate of a purely elastic solid. In common materials the situation is much more complicated. Nevertheless this concept of Griffith is generally accepted nowadays and forms the basis of almost any fracture theory. The problem that remains is how to describe the criteria for nucleation and propagation of a crack in a real solid. In a more general approach based on continuum mechanics, as initiated by Irwin [16] and Orowan [17], this leads to a modification of the Griffith formula:

$$\sigma = (G_{IC}E/Y^2c)^{1/2} \qquad (2)$$

As compared to the Griffith equation the surface energy of the two newly created surfaces in the crack, 2γ, is replaced by G_{IC}, the energy required to grow a crack of critical dimensions. This term G_{IC}, which includes all sorts of dissipative energy contributions that occur in the crack opening process, may be several times larger than the surface energy. Also the factor π in the Griffith equation is replaced by a term Y^2, which corrects for the geometrical dependence of the strength. As a matter of fact $Y^2 = \pi$ in the case of a crack being formed in a plate of infinite dimensions [18]. In different geometries, however, Y^2 has another value and standards methods have been developed for the determination of the dependence of Y^2 on crack length and specimen dimensions in pre-cracked specimen [18]. Values of Y^2 in specific geometries have been tabulated [19, 20].

One should realize that this continuum approach to the fracture process is purely phenomenological and does not take into account any molecular interpretation of the fracture process. Fracture theories based on a molecular approach of the breaking events in polymers try to give an explanation for the time and temperature dependence of the strength. This phenomenon was first theoretically interpreted by Tobolsky and Eyring [21] as fracture being a thermally activated rate process. Since then a number of theories were developed considering the lifetime of polymers under stress, each of them, based on quite different molecular interpretations of the fracture process.

By far the most widely used expression for the lifetime as a function of stress was given by Zhurkov [22] and Zhurkov and Korsukov [23],

$$t_b = t_0 \exp[(U_0 - \gamma\sigma)/kT] \quad (3)$$

with t_b is time to break, σ is tensile stress, U_0 is bond dissociation energy, $t_0 = 1/\nu$, with ν being the frequency of atomic vibrations, and γ is a coefficient depending on the actual stress on the bonds, i.e. the activation volume of the bond.

The Zhurkov model is founded on the scission of primary bonds in the polymer chain, which leads to the formation of submicrocracks, which either coalesce or develop into larger cracks. The breakage of primary bonds in the fracture process was experimentally confirmed by electron paramagnetic resonance (EPR) measurements [24], revealing the generation of a great number of radicals in polymeric samples under the action of mechanical stresses. The formation of microvoids in polymers under uniaxial tension could be observed experimentally with small angle X-ray spectroscopy (SAXS), which showed that such voids all have more or less the same dimensions [25].

Nevertheless there have been some objections to Zhurkov's view on the fracture process in polymers [26, 27]. It is true that EPR measurements have shown that in a strained polymer sample, even before fracture has occurred, many more radicals are generated than the maximum number of chains that can be ruptured at the fracture surface, but it has also been shown that the radicals occur uniformly throughout the sample [24, 28]. As compared to the number of chains per unit volume only a small fraction of the polymer chains was broken. Apart from this, it was noticed that after fracture occurred, the unbroken part showed no decline of strength in a second run, although no new chains were broken [29]. These results already indicate that fracture does not necessarily proceed entirely by primary bond breakage and furthermore that breakage of bonds need not be the rate determining step in failure, but far more so the growth of cracks to their critical dimensions. Zhurkov considers the initial fracture of bonds to form a microcrack as the rate determining step and ignores the time needed for the propagation of the crack. Besides, if indeed crack opening and growth is the main event in fracture, one could expect the lifetime of the polymer to depend on σ^2, instead of σ, since the propagating steps in crack opening would be governed by the strain energy $\sigma^2/2E$, especially in the case of highly extended molecules [30, 31]. These considerations were taken into account in a model by Prevorsek and Lyons [32] and Prevorsek [33], who assumed that failure proceeds by the nucleation and propagation of circular flaws, throughout the sample. Another assumption concerns the propagating step, which is believed to be governed by the strain energy $\sigma^2/2E$. The fracture path will seek the energetically most favourable way, i.e. both chain scissioning and chain slippage, depending on what is most favourable. This leads to the following expression for the lifetime under the action of a constant tensile stress σ:

$$t_b = (h/kTZV) \times \exp(\Delta f_r^*/kT + \Delta F^{\ddagger}/kT - vq^2\sigma^2/2EkT) \quad (4)$$

where t_b is time to break, σ is the tensile stress, E is the crystal modulus, v is activation volume, $\Delta F^{\ddagger}$ is activation energy for crack growth, governed by primary and secondary bond breakage, Δf_r^* is free energy associated with the formation of a crack, V is the volume of the specimen, Z is the concentration of nucleation sites and q is a stress concentration factor.

Also the Prevorsek approach has been criticized [31], since it assumes the formation of circular cracks throughout the sample. Observations on crack formation generally point to the presence of long narrow cracks, which appear to be mainly located at the surface of a sample [31, 34]. The cracks being non-circular, could be accounted for in the above given expression by a different value of the stress concentration factor q, which also corrects for the fact that most polymers have a highly heterogeneous structure and cannot be regarded as a continuum. Apart from this, the term $\Delta f_r^*/kT$ would be affected, but at moderate stresses this term can be neglected, since it is proportional to σ^{-4}. However, a different distribution of cracks throughout the sample, i.e. cracks being formed at the surface, would make it necessary to modify the pre-exponential factor in Equation 4 substantially.

Finally it has been supposed that polymer fracture proceeds mainly by the breaking of intermolecular bonds [35, 36]. Molecular rearrangements which take place under the influence of stress thus would determine the time to failure. The expression for the lifetime in polymeric samples as given by Coleman [35] and Coleman and Knox [36] is

$$t_b = (\gamma_b h/\lambda kT) \exp(\Delta F^*/kT - A\lambda\sigma/2kT) \quad (5)$$

In this expression γ_b/λ is the number of molecular jumps to failure, ΔF^* is the activation energy for creep and A is the cross-sectional area of the chain in the crystal lattice and λ is the C–C bond distance. Obviously this model ignores many observations on radical formation in polymers under tensile stress.

Although none of these lifetime models apparently is able to explain the complete failure behaviour in polymers, it could very well be that they are applicable under certain circumstances. This is because the fracture mechanism in polymers under tensile stress is dependent on a broad range of conditions, such as the chemical structure and morphology of the polymer, its molecular weight, the orientation of the molecules, their resistance to flow, time, temperature, the presence of impurities, structural defects, trapped entanglements, etc. For this reason the lifetime data obtained on highly oriented UHMWPE were evaluated according to each of the three lifetime models presented above.

Many additional aspects of the complex fracture process have been dealt with in excellent reviews given by Andrews [30], Williams [18], Krausz and Eyring [37], Kausch [38] and Peterlin [27].

3. Experimental details

The linear polyethylene used was Hi-fax 1900, with a weight average molecular weight $\bar{M}_w = 4 \times 10^6$ and a number average molecular weight $\bar{M}_n = 2 \times 10^5$. The preparation of the gel-spun and hot-drawn polyethylene fibres has been described in detail elsewhere [7, 8]. The fibres were spun from 5 wt% solutions of Hi-fax in paraffin-oil, after which the filaments were extracted with *n*-hexane. The porous fibres, thus obtained, were subsequently hot-drawn at a drawing temperature of 148° C.

The crosslinked UHMWPE fibres were prepared by soaking a porous as-spun fibre in dicumylperoxide, until it absorbed so much peroxide, that the filament contained 50 wt% peroxide. In a subsequent stage the fibre was hot-drawn to a draw ratio of 20 at 100° C and thereafter to a draw ratio of 2.5 at 160° C. A more detailed description of this procedure is given elsewhere [39].

The poly(*p*-phenyleneterephtalamide) fibres were multifilaments kindly supplied by the ENKA Research Institute (Arnhem, the Netherlands).

Cross-sectional areas of the filaments were determined from fibre weight and length assuming a density of 1000 kg m^{-3} for polyethylene and 1450 kg m^{-3} for the aramid. For the lifetime measurements a piece of fibre of 25 cm in length was clamped at both ends. One of the clamps had a fixed position, whereas the other was freely suspended to which different weights were attached. An electrically heated oven was employed to achieve temperatures above ambience. Basically it consisted of two heated brass plates leaving a small cavity when pressed together, in which the sample was placed. The device was thermally insulated with polyurethane foam, which made that the temperature in the oven could be regulated within 1° C. The clamping occurred outside the oven. Normal tensile testing of the fibres was carried out on a Zwick Z1 3B tensile tester at a crosshead speed of 12 mm min^{-1} and an original sample length of 25 mm. Scanning electron microscopy was performed with an ISI-DS 130 microscope operated at 40 kV on gold covered samples.

4. Results and discussion

4.1. Lifetime measurements at various temperatures

To determine the activation energy associated with the fracture process, lifetime measurements in dead-load tests have been performed on the gel-spun and hot-drawn UHMWPE fibres at various temperatures. Fig. 1 presents a plot of the logarithm of time to break ln t_b as a function of the nominal tensile stress σ_0 at temperatures between 25 and 140° C for a gel-spun UHMWPE fibre, that was hot-drawn at 148° C [7, 40] to a draw ratio of 90. This fibre had a tensile strength at break of 3.5 GPa in normal tensile testing (tensile speed 12 mm min^{-1}, sample length 25 mm, temperature 20° C). Straight lines were obtained for the ln $t_b - \sigma_0$ behaviour at temperatures up to 100° C as to be expected according to the lifetime models of Zhurkov [22], Zhurkov and Korsukov [23], Coleman [35] and Coleman and Knox [36].

The lifetime measurements at temperatures above 100° C were accompanied by a significant length increase of the filaments from about 30% at 120° C to more than 100% at 140° C. Also in conventional tensile testing of the UHMWPE fibres Torfs [41] noticed that especially at temperatures above 100° C extensive yielding occurred, leading to large elongations at break. Hence the fracture of the UHMWPE fibres in this temperature range

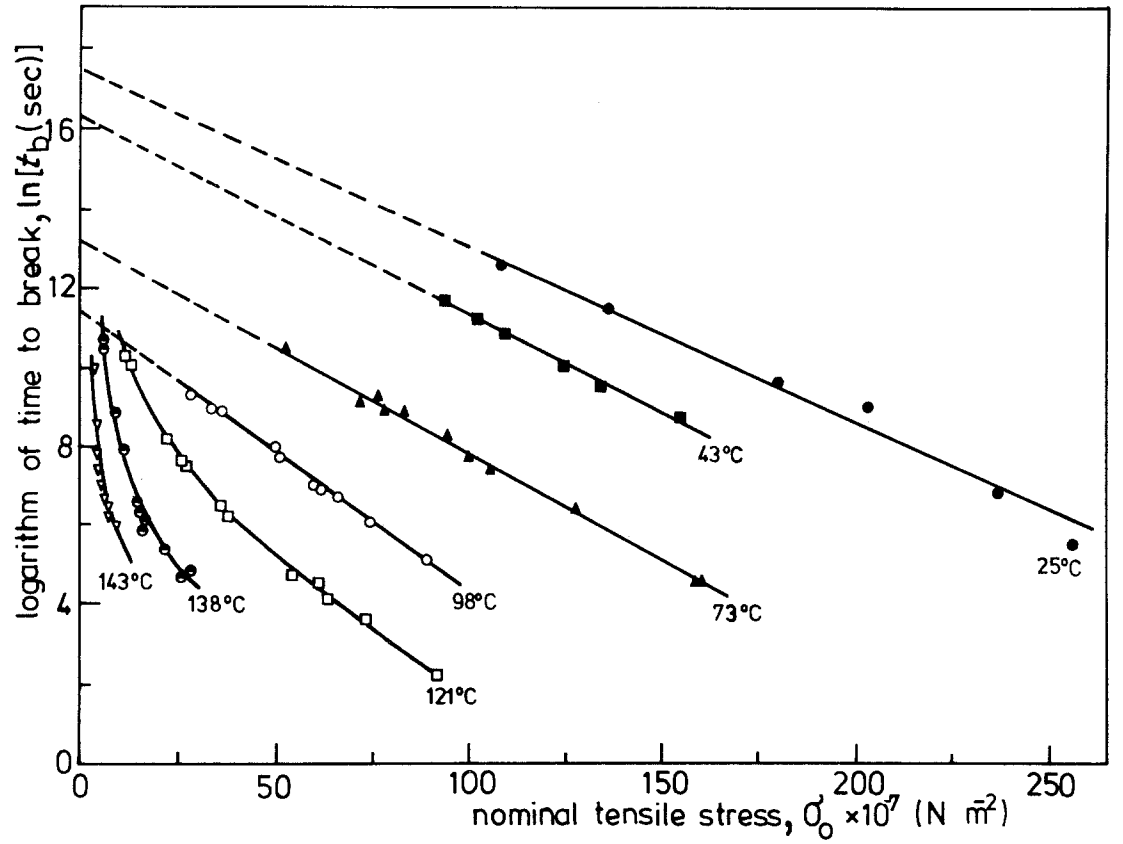

Figure 1 Lifetime as a function of nominal tensile stress σ_0 at various temperatures for a gel-spun and hot-drawn UHMWPE fibre, which had a strength of 3.5 GPa in normal tensile testing.

is likely to proceed by creep failure, although some primary bond breakage may be involved, since already in the hot-drawing of the UHMWPE fibres some molecular breakdown occurred [42]. This creep behaviour is reflected in the lifetime behaviour by a non-linearity of the $\ln t_b - \sigma_0$ curves. This curvature in the $\ln t_b - \sigma$ behaviour at temperatures above 100° C in Fig. 1 would have been even stronger if the true stress at break had been plotted, since we noticed that in this high temperature range the elongation at break was also dependent on the applied stress. Fig. 2 shows

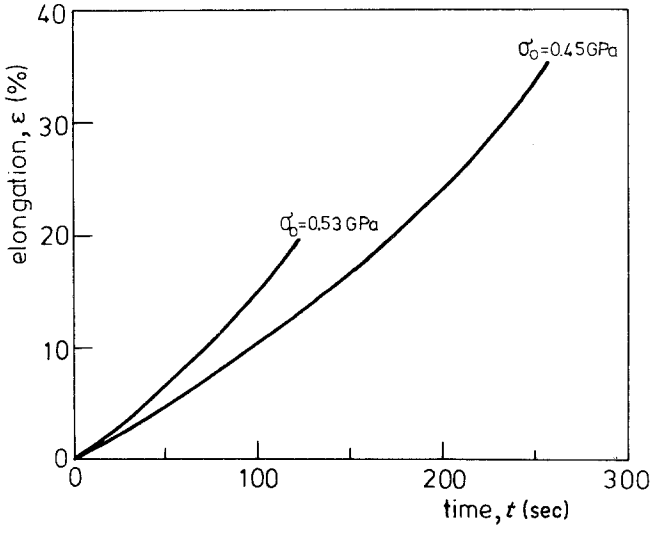

Figure 2 Elongation against time during lifetime experiments at 121° C under the action of nominal stresses of 0.45 and 0.53 GPa.

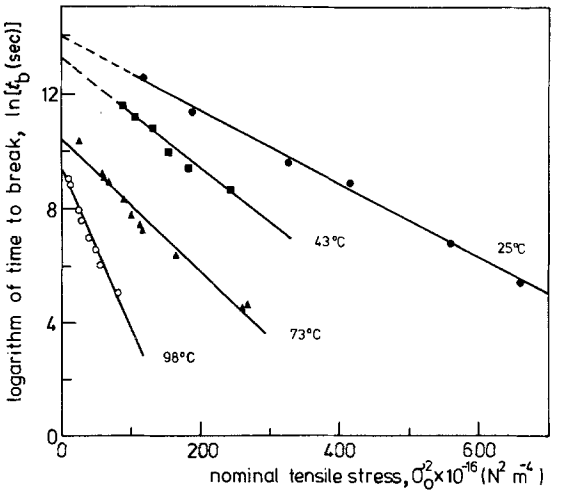

Figure 3 Dependence of logarithm of time to break $\ln t_b$ on the second power of nominal tensile stress σ_0^2.

the elongation as a function of time at 121° C at nominal stress values of 0.45 GPa and 0.53 GPa. It can be seen that the elongation changes continuously with time to 18% at a nominal stress of 0.53 GPa and 32% at 0.45 GPa nominal stress.

Accordingly it would be meaningless to analyse these high temperature lifetime data with the lifetime models presented in Section 2, since they require the stress to be constant throughout the measurements. That is why only the data obtained at temperatures below 100° C were used to investigate the applicability of these models, although also in this temperature interval the elongation at break increased from 3.2% at 25° C, 4.5% at 43° C, 8.7% at 73° C to 18.0% at 98° C. The nominal stress values as shown in Fig. 1 were corrected for these elongations, using

$$\sigma = \sigma_0(1 + \epsilon) \qquad (6)$$

with σ_0 is nominal stress and ϵ is elongation at break. Strictly spoken, such a correction only makes sense, if most of the stretching occurs in a time interval which is very much smaller than the breaking time t_b [35], which according to Fig. 2 was not the case. Nevertheless this approach seemed acceptable, since the calculated values of the activation energy and the pre-exponential factor in the lifetime models of Zhurkov, Coleman and Prevorsek were almost unaffected by these corrections.

As already pointed out in Section 2, the Prevorsek model predicts a linear relationship between $\ln t_b$ and σ^2. In Fig. 3 the $\ln t_b$ data are replotted against σ_0^2, which also gives good agreement with linear relationships in the temperature range up to 100° C. Therefore none of the three models can be excluded at forehand and the lifetime data were evaluated according to each of the models, to establish which one fits best to the fracture process in the UHMWPE fibres.

To estimate the activation energy from the Zhurkov Equation 3 the $\ln t_b - \sigma$ curves were extrapolated to stress zero, using a least squares analysis. Subsequently the extrapolated values of $(\ln t_b)_{\sigma=0}$ were plotted against the reciprocal of absolute temperature $1/T$ as depicted in Fig. 4a. From the slope of the straight line, thus obtained, the activation energy $U_0 = 76\,\mathrm{kJ\,mol^{-1}}$ is found and the intercept gives for the pre-exponential factor $t_0 = 2.2 \times 10^{-6}$ sec. Basing on the Coleman formula (Equation 5), extrapolation of the $\ln t_b - \sigma$ lines to $\sigma = 0$ leads to an intercept $I = \ln(\gamma_b h/\lambda kT) + \Delta F^*/kT$. A plot was made of $x = I - \ln(h/kT)$ against $1/T$ in Fig. 4b, from which the activation energy was found to be $\Delta F^* = 73\,\mathrm{kJ\,mol^{-1}}$ and the number of jumps to failure $\gamma_b/\lambda = 4.2 \times 10^7$. The Prevorsek equation (Equation 4) gives as an intercept after extrapolation of the $\ln t_b - \sigma^2$ lines to $\sigma = 0$, a value of $I = \ln(h/kTZV) + \Delta F^{\ddagger}/kT$. Subsequently plotting of $x = I - \ln h/kT$ against $1/T$ in Fig. 4c, yields for $\Delta F^{\ddagger} = 62\,\mathrm{kJ\,mol^{-1}}$ and for the number of nucleation sites $Z = 2.5 \times 10^{-5}\ \mathrm{cm^{-3}}$.

Table I summarizes the values found for the activation energy, the pre-exponential factor and the activation volume at 25° C in the three equations. For the determination of the activation

TABLE I Experimental values of activation energy, activation volume (25° C) and pre-exponential factor according to the lifetime equations of Zhurkov (Equation 3), Coleman (Equation 5) and Prevorsek (Equation 4)

Failure model	E_a (kJ mol^{-1})	Activation volume (nm^3)	Pre-exponential factor	Theoretical value of pre-exponential factor
Zhurkov	76	0.018	$t_0 = 2.2 \times 10^{-6}$ sec	$t_0 = 10^{-12}$ to 10^{-13} sec
Coleman	73	0.036	$\gamma_b/\lambda = 4.2 \times 10^7$	$\gamma_b/\lambda = 1$–10
Prevorsek	62	0.030	$Z = 2.5 \times 10^{-5}\ \mathrm{cm^{-3}}$	$Z \approx 10^{16}\ \mathrm{cm^{-3}}$

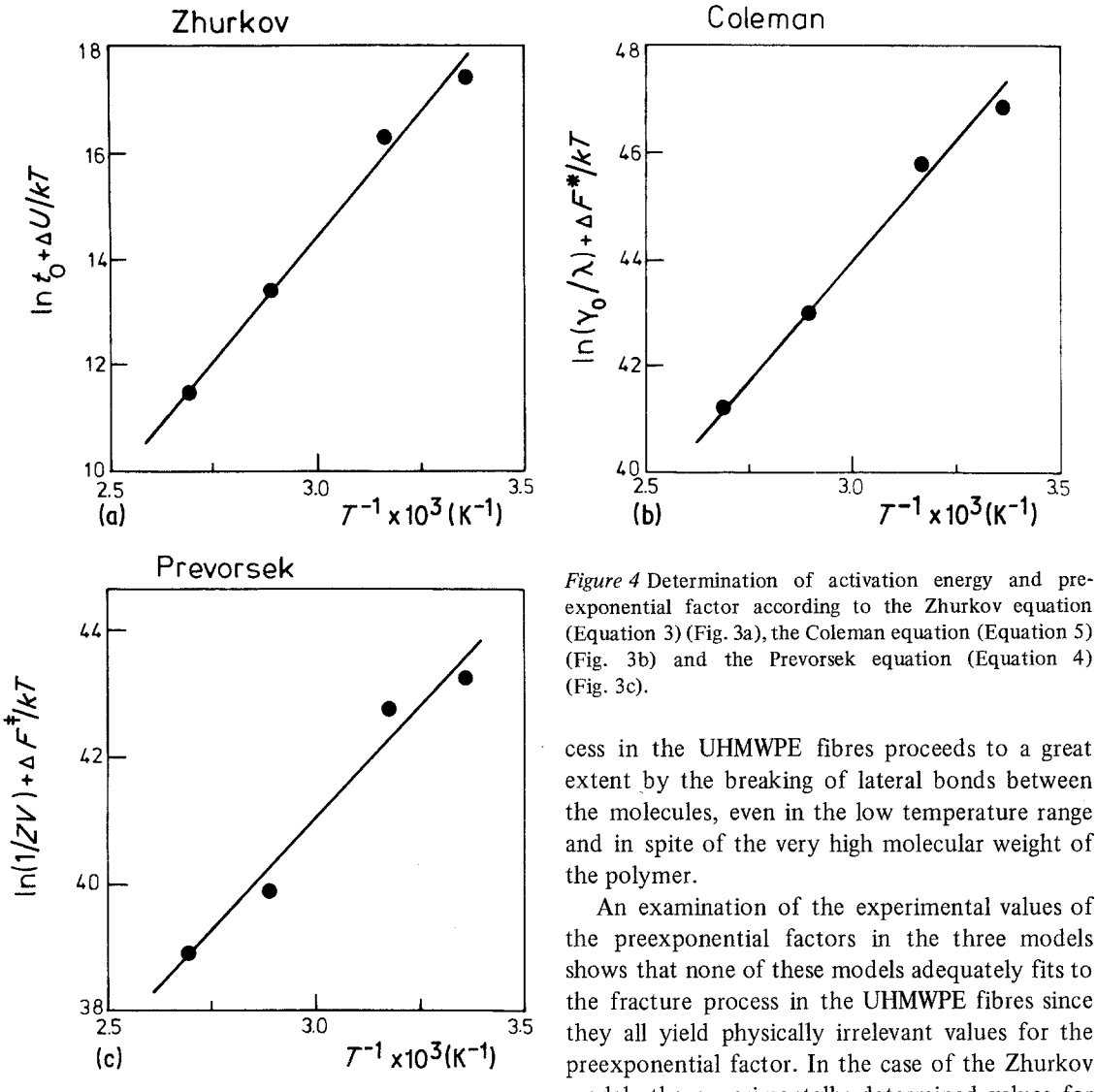

Figure 4 Determination of activation energy and pre-exponential factor according to the Zhurkov equation (Equation 3) (Fig. 3a), the Coleman equation (Equation 5) (Fig. 3b) and the Prevorsek equation (Equation 4) (Fig. 3c).

volume in the Prevorsek equation (Equation 4) a value for the stress concentration factor q of 10 was used [32] and for the crystal modulus E a value of 300 GPa [43].

In spite of the fact that the three models are based on quite different views on the molecular fracture events, they all yield about the same value for the activation energy of 60 to 75 kJ mol^{-1} in the highly oriented UHMWPE fibres. This magnitude of the activation energy is very much lower, than the bond energy of the C–C bond in polyethylene, which is about 300 kJ mol^{-1} and also significantly lower than the value of 113 kJ mol^{-1} estimated by Zhurkov [23] for the dissociation energy in polethylene under tensile stress. This quite clearly demonstrates that the fracture process in the UHMWPE fibres proceeds to a great extent by the breaking of lateral bonds between the molecules, even in the low temperature range and in spite of the very high molecular weight of the polymer.

An examination of the experimental values of the preexponential factors in the three models shows that none of these models adequately fits to the fracture process in the UHMWPE fibres since they all yield physically irrelevant values for the preexponential factor. In the case of the Zhurkov model, the experimentally determined values for t_0, the reciprocal atomic vibration frequency, was 2.2×10^{-6} sec, which is quite different from $t_0 = 10^{-12}$ to 10^{-13} sec, what it should be [22, 23]. The same holds for the Coleman expression (Equation 5), where we estimated a value for γ_b/λ, the number of jumps to failure of 4.2×10^7, which is meaningless since it is even much larger than the average number of C–C distances, the single jump distance [2], in a molecule of about 1.4×10^4. For the number of nucleation sites Z, in the Prevorsek equation (Equation 4), a value of 2.5×10^{-5} cm^{-3} was found, which has no significance at all, as compared to a number of crystallites of about 10^{16} cm^{-3} in the UHMWPE fibres. According to Prevorsek [33] a potential nucleation site resides in the boundary regions between the crystallites.

Conclusively these models can qualitatively describe the failure process in the UHMWPE fibres as far as the $\ln t_b - \sigma$ behaviour is concerned, but do not give a quantitative agreement with any physical interpretation of the fracture process. Therefore additional investigations were undertaken to get a better insight in the failure behaviour of the gel-spun and hot-drawn UHMWPE fibres.

4.2. Lateral bonding

The dominant role of the lateral bonding between the polyethylene chains in determining the strength properties is further elucidated in Fig. 5. It depicts the logarithm of time to break $\ln t_b$ as a function of tensile stress σ at 25° C for the gel-spun and hot-drawn UHMWPE fibres, used in obtaining Fig. 1, as compared to the lifetime behaviour of oriented poly(*p*-phenyleneterephtalamide) fibres (Arenka) and a UHMWPE fibre, that was prepared by simultaneous hot-drawing and crosslinking with di-cumylperoxide.

The Arenka fibres are much more capable of sustaining significant loads for an extended period of time than the gel-spun and hot-drawn fibres. If strength were to be determined entirely by covalent bond strength in the polyethylene chains, one would not expect such a large difference in the lifetime behaviour, since the bond energy in polyethylene and poly(*p*-phenyleneterephthalamide) is of the same order of magnitude. This large

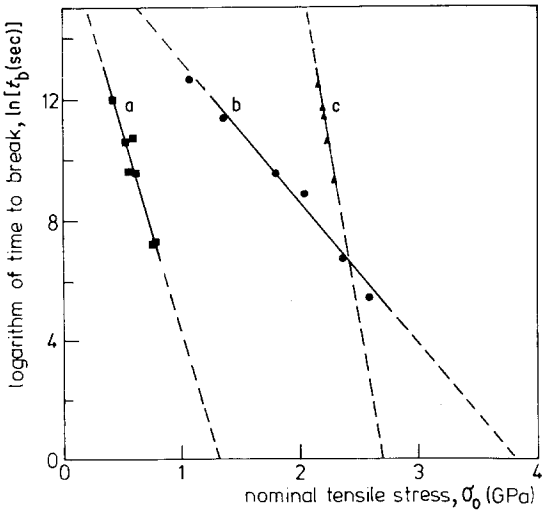

Figure 5 Lifetime determination in constant load tests at room temperature for a crosslinked gel-spun and hot-drawn UHMWPE fibre (a), a non-crosslinked gel-spun and hot-drawn UHMWPE fibre (b) and poly(*p*-phenyleneterephtalamide) multifilament (c).

difference in lifetime behaviour must be due to the cohesive forces between the polymer chains, since in polyethylene only van der Waals bonds are present, whereas in the aramid fibres the lateral cohesion between the rigid chains comes from strong hydrogen bonding. Following this line of reasoning the lifetime behaviour of the UHMWPE fibres must be substantially changed if the molecules were connected to each other by chemical crosslinks [39], as is indeed the case according to Fig. 5. Due to the chemical crosslinking during the hot-drawing of the UHMWPE fibres, the ultimate strength of the fibre was reduced from 3.5 GPa to about 1.5 GPa. This reduction can be attributed to the restricted drawability as a consequence of introducing chemical crosslinks, which will also act as stress concentrations in the crystal lattice. Apart from this some contamination of the polyethylene chains takes place by cumuloxy groups due to side reactions in the crosslinking process [44].

The presence of foreign impurities in a fibre can strongly affect the strength. It has been noticed in the preparation of carbon fibres by carbonization of polyacrylonitrile (PAN) fibres that the strength increased from 1 to 3 GPa, if in the initial stages of preparation the PAN solutions had been filtrated [45].

If we now return to the lifetime behaviour of the crosslinked UHMWPE fibre, we observed that the time to break in this fibre increases much faster with decreasing stress than for the non-crosslinked fibre. This must be caused by the fact that the chains are connected to each other by covalent bonds. Consequently one could expect these crosslinked fibres to obey the Zhurkov formula (Equation 3) for the lifetime, since this formula is based on primary bond breakage. Indeed, if one applies the Zhurkov formula to the lifetime behaviour in the crosslinked fibre, inserting a value of $113\,\mathrm{kJ\,mol^{-1}}$ for the activation energy as estimated by Zhurkov and Korsukov [23] in polyethylene, a pre-exponential factor $t_0 = 1.7 \times 10^{-12}$ sec is found. This value for t_0 is fully in accordance with the Zhurkov model and shows that fracture in the crosslinked UHMWPE fibre proceeds by covalent bond breakage.

An interesting question that now comes up is, how the different fracture mechanisms in the crosslinked and non-crosslinked UHMWPE fibres manifest themselves in the macroscopic appearance of the fracture surfaces. This will be dealt with in the next section.

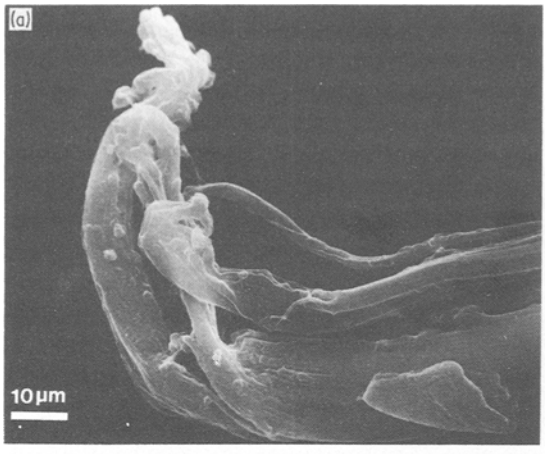

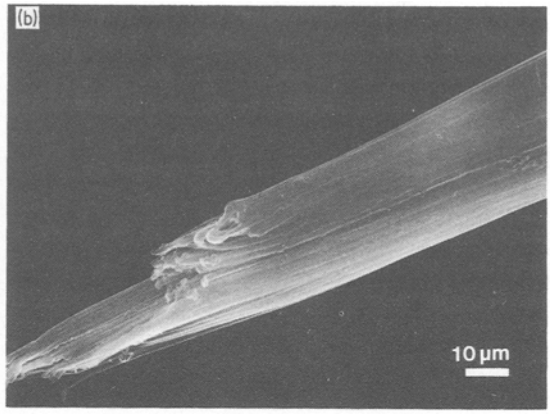

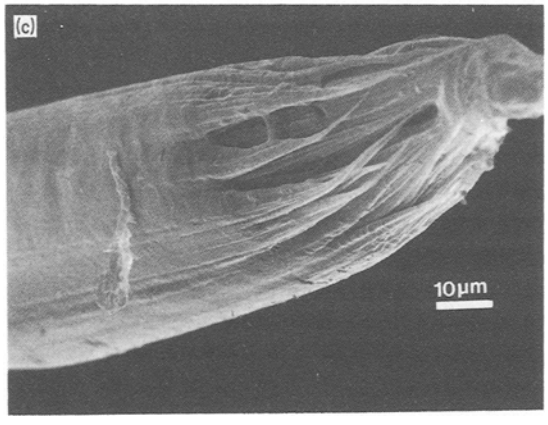

Figure 6 (a) SEM micrograph of the fracture surface in a non-crosslinked UHMWPE fibre subjected to normal tensile testing at room temperature. (b) SEM micrograph of the fracture surface in a non-crosslinked UHMWPE fibre after a constant load test at 73° C and a nominal stress $\sigma_0 = 0.37$ GPa. (c) SEM micrograph of the fracture surface in a non-crosslinked UHMWPE fibre subjected to a nominal stress of 0.06 GPa at 138° C.

4.3. Morphological appearance of the fracture process

Fig. 6 presents some SEM micrographs of the fracture surfaces of the non-crosslinked highly oriented UHMWPE fibre after fracture under different circumstances. Fig. 6a was obtained after fracture in normal tensile testing at 20° C and a tensile speed of 12 mm min^{-1}. Fig. 6b discloses the fracture surface after a dead load test at 73° C and a nominal stress of 0.37 GPa, whereas Fig. 6c comprises the fracture surface after a dead-load test at 138° C and a nominal stress of 0.06 GPa. In all cases a highly fibrillated fracture surface is disclosed. In the sample broken at the highest temperature of 138° C it can be seen that after fracture partial melting of the fibrils occurred, due to the release of the constraints on the fibre. The melting temperature of the UHMWPE fibres is significantly raised, if shrinkage is prevented by keeping them at constant length [46].

The appearance of the fracture surfaces in the cross-linked UHMWPE fibre was quite different. Fig. 7 displays a SEM micrograph of the fracture surface in the crosslinked fibre after a dead load test at 25° C and a stress of 0.77 GPa. This fracture surface which was clearly initiated at an impurity, indicates brittle failure. Another remarkable feature of Fig. 7 is, that no fibrillation can be discerned in the crosslinked fibre. Apparently due to the chemical crosslinking, fibrillation is avoided in the hot-drawing process, which leads to a brittle fracture behaviour.

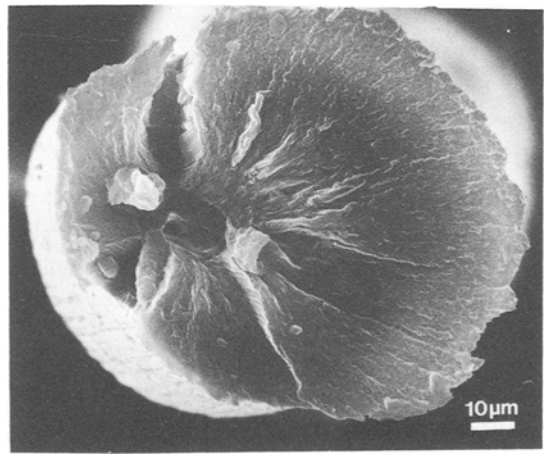

Figure 7 Fracture surface in a crosslinked UHMWPE fibre after a dead load test at 25° C and a nominal stress of 0.77 GPa.

Consequently the noteworthy contribution of molecular slippage to the failure in the non-crosslinked fibres must be associated with the presence of a fibrillated structure in such fibres. The fibrillated fracture surfaces point to a fracture mechanism very similar to the one proposed by Peterlin [47]. Crack formation in the fibrillated UHMWPE fibres presumably proceeds by cutting through a fibril at a weak spot, i.e. a defect region, after which the crack easily grows further along the boundary of the fibril, until it meets a defect region in the neighbouring fibril, etc. Accordingly crack growth would be a step wise process of cutting through fibrils at defect regions and breaking of lateral bonds between fibrils. Such a mechanism is also consistent with the observation as revealed by SAXS, that under the action of uniaxal tension, microvoids are generated in oriented polymers [25]. Such microvoids all have about the same dimensions, whereas their number steadily increases with time. The lateral dimensions of such microvoids were found to be about 15 to 20 nm in polyethylene, which about equals the generally observed diameter of the fibrillar entities. Preliminary investigations on the gel-spun and hot-drawn UHMWPE fibres by SAXS also pointed to the generation of such microvoids [48].

The defect regions in the fibrillar structure where the microvoids are likely to be formed are the ends of the very long fibrils [8, 47] as well as several regions in the fibrillar entities with a high topological defect concentration, such as trapped entanglements and chain ends. These topological defect regions in the fibrillar entities originate from the flow units that were initially formed in the spinning solution during the gel-spinning of the UHMWPE. In the flow field during spinning the entanglement network in the UHMWPE solutions splits up in long bundle-like flow units, consisting of alternating bundles of elongated molecules, which are connected by entanglements to large clusters of unoriented molecules [8]. These clusters comprise highly entangled aggregates of elastically inactive loops, dangling chains and a few tie molecules. Solidification of this structure after spinning yields a morphology of large lamellae interconnected by several fibrils. Hot-drawing converts this morphology into a smooth fibrillar structure, during which the elastically inactive loops and chain ends of the original lamellae are transformed into chain extended fibrillar material by elongating them between the original short fibrillar entities. Drawing is completed if the loose molecules are fully elongated between entanglements. It follows, therefore, that in the fully oriented fibres after hot-drawing the fibrillar entities still contain defect regions, encompassing trapped entanglements and chain ends. These topological defect regions must make up the weak spots in the fibrils where a growing crack passes through.

This suggestion that the strength of the UHMWPE fibres is determined by the presence of topological defects, is also consistent with some annealing experiments on the fibres. It is well known that annealing can improve the crystal structure, due to migration of (point) dislocations towards the ends of the molecules [49, 50]. Annealing of the UHMWPE fibres at constant length just below the melting temperature, leaves the strength however unaffected. The strength is thus not determined by dislocations in the crystal lattice, but far more by topological defects as trapped entanglements and chain ends, which cannot be removed upon annealing. A possible method to attack the trapped entanglements in the crystal lattice is by annealing under high pressure. Since entanglements represent bulky space elements in the polymer chain, disturbing the crystal lattice, the molecules will be cut at these sites under elevated pressure. Indeed we noticed after annealing at a pressure of 6.2 kbar and a temperature of 245° C, that the strength of the UHMWPE fibres was significantly decreased, whereas the crystallinity increased [51], due to the scissioning of molecules at entanglement sites [52, 53].

All these observations clearly suggest that fracture in the gel-spun and hot-drawn fibres occurs by cutting through fibrils at topological defect regions. The breakage of the individual fibrils presumably proceeds by a combined process of chain rupture, e.g. tie molecules and heavily entangled molecules, and molecular slippage, leading to disentangling of molecules, which have short chain ends protruding from the entanglements [47, 54, 55]. In this process the contribution of molecular slippage and not to forget slippage of fibrils past each other gradually increases as the temperature rises, especially at temperatures above 100° C, where extensive yielding takes place. A clear indication for the dominancy of creep failure at high temperatures is revealed by the fracture surface in Fig. 6c where the broken

fibrils have very sharp tapered ends. A possible explanation for the increasing contribution of creep failure, especially at high temperature has been given by Torfs [41]. He proposed that the process of creep failure might be associated with a shift of a phase transition in the highly oriented UHMWPE from the orthorhombic to a hexagonal phase. This hexagonal phase, which is characterized by a high molecular mobility, is usually encountered in the UHMWPE above 150° C [46]. Torfs [41] suggested that this phase transition can be shifted to lower temperatures under the action of a tensile stress [56]. It would mean in a dead-load test that under the action of the tensile stress some material is transformed into the hexagonal phase, in particular in the neighbourhood of structural defects, where stress concentrations occur. This leads to failure of this fraction of material and consequently the stress on the remaining part increases, which then gradually transforms until the stress reaches the level that all the material is transformed into the hexagonal phase, after which the fibre fails in a dramatic way.

4.4. Surface flaws

In the previous section it has been pointed out how a growing crack finds its way through the highly oriented UHMWPE filaments. A problem that remains to be solved is where such cracks are initiated, i.e. what irregularities in the fibre structure cause the beginning of a crack. In many fibre substances it has been noticed that crack formation is associated with the presence of surface imperfections [9, 34, 57]. Electron microscopical investigation of the surface of the UHMWPE fibres revealed the presence of kink bands as displayed in the SEM micrograph of Fig. 8. It was recently recognized by Pelzbauer and co-workers [58] that such kink bands in polyethylene cause stress concentrations where cracks are preferentially being formed. Also the strength of poly-diacetylene whiskers has been related to the presence of surface steps [59]. This view is corroborated by the finding that the highly oriented UHMWPE fibres were preferentially attacked at these kink bands if they were exposed to chlorosulphonic acid HSO_3Cl. Fig. 9 presents a SEM micrograph of a fibre that was exposed to chlorosulphonic acid for 45 min at 80° C. Fibrils were broken all around the fibre in the direct vicinity of a kink band. More severe etching of the fibres leads to the formation of complete circumferential cracks,

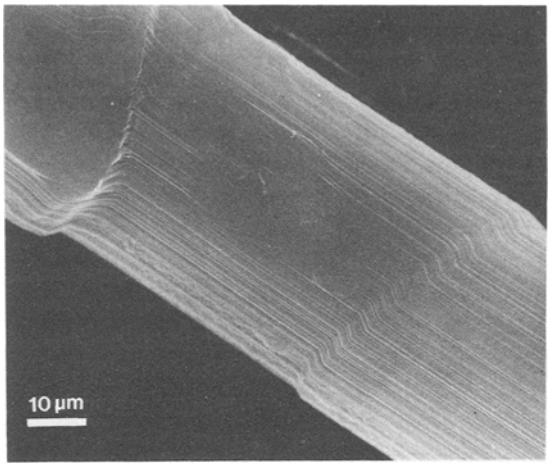

Figure 8 SEM micrograph of the surface of a highly oriented gel-spun and hot-drawn UHMWPE fibre revealing kink bands.

which penetrate from the surface to the interior of the fibre. An example of such cracks, in which a fibrillated fracture surface is encountered, is shown in Fig. 10, which comprises a SEM micrograph of a fibre after treatment with chlorosulphonic acid for 30 min at 100° C. There is a striking resemblance with the "onion-skin" effect in polyethylene fibres as observed by Nadkarni and Schultz [60] and the perpendicular cracks observed in cold drawn polyethylene by Jarecki and Meier [57].

We noticed that thicker filaments generally displayed more kink bands than thinner ones. This phenomenon clearly must be related to the origin of kink band formation. The question however is where the compressive forces needed for

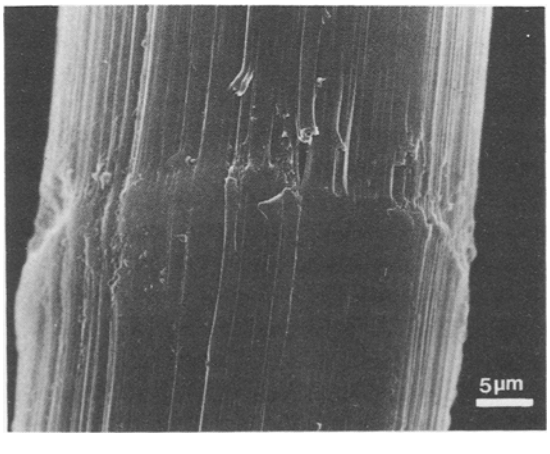

Figure 9 SEM micrograph of a UHMWPE fibre exposed to chlorosulfonic acid for 45 min at 80° C.

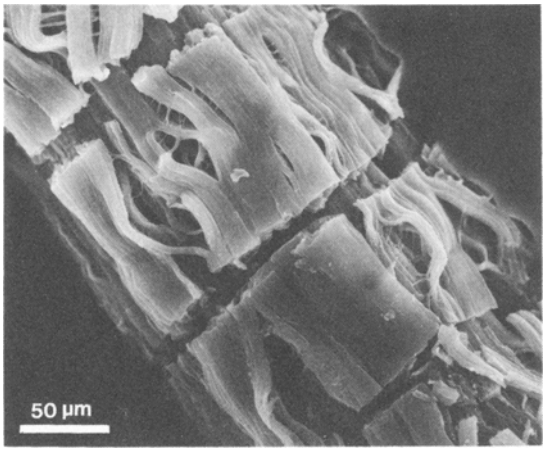

Figure 10 SEM micrograph of a highly cracked filament due to a treatment with chlorosulphonic acid for 30 min at 100° C.

the kinking come from. It has been pointed out that the stress concentrations needed for the formation of kinks are likely to be located at the ends of the fibrils [58]. Presumably the kink bands are developed in the early stages of hot-drawing of the UHMWPE fibres where a complex process of combined heat and mass transfer takes place. If the fibre enters the drawing apparatus it is heated and deformed simultaneously. Consequently the outer layer of the fibre first reaches the drawing temperature, where the flow begins. Only thereafter the interior of the fibre is heated through and loses its resistance to elongation of the molecules in the flow units.

Under these circumstances thermal and compressive stress may be generated in the filament in addition to the applied drawing stress, which make that drawing proceeds initially by shearing of concentric cylindrical layers past each other, similar to the drawing out of a telescope. In the course of this process the kink bands are formed. This effect will be stronger as the filaments become thicker, since it takes longer for these filaments to be heated through. Consequently thicker fibres contain more of these surface flaws. If indeed these surface imperfections, i.e. the kink bands, are responsible for the initiation of cracks in the loaded specimen, one could expect the strength of the UHMWPE fibres to be dependent on their diameter. Not only the number of surface flaws becomes less with decreasing diameter, but also the amount of elastic energy, gained from the surrounding of a crack. This energy which is needed to bring up the fracture surface energy, is limited in thin filaments due to the stronger curvature of its surface. Fig. 11 presents a plot of the tensile strength at break in normal tensile testing of fully oriented UHMWPE fibres as a function of their diameter. The data of Fig. 11 were obtained on fibres produced by the surface growth technique [4, 5], which were subsequently hot-drawn and on gel-spun fibres, that were all spun under similar conditions and subsequently hot-drawn to the maximum draw ratio in the range of 50 to 100. The strength of the UHMWPE fibres indeed decreases with increasing diameter. Quite similar behaviour has been observed for the strength of polydiacetlyene whiskers [59] and glass-fibres [9]. As far as we know such a strong dependence of fibre strength on diameter has never been observed in polymeric fibres. This is

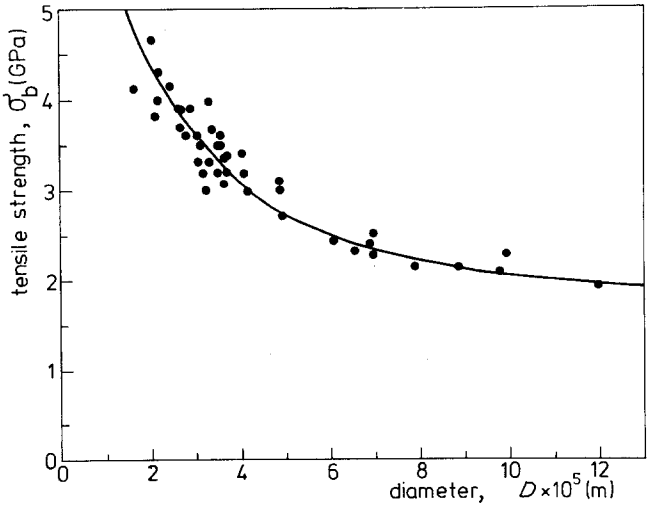

Figure 11 Tensile strength at break σ_b for fully oriented polyethylene filaments as a function of fibre diameter.

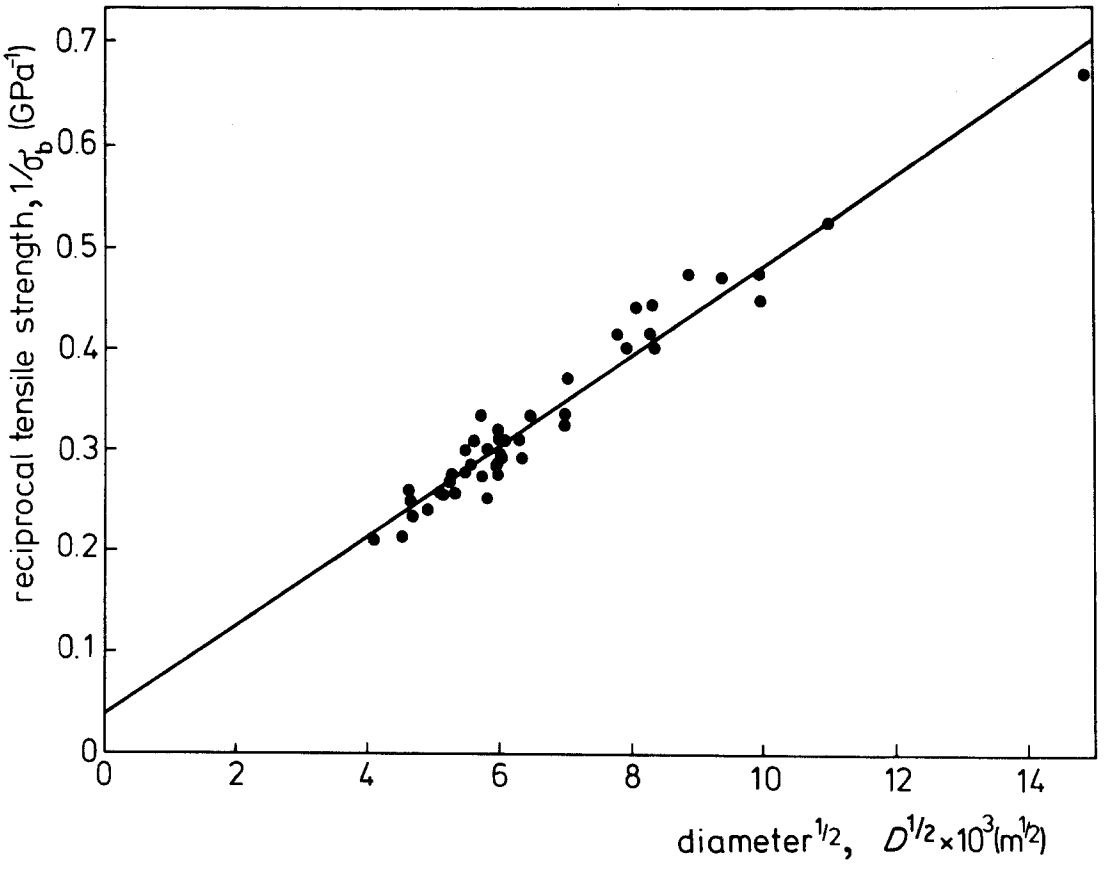

Figure 12 Linear strength-diameter relationship as observed for the fully oriented UHMWPE filaments.

probably due to the fact that common polymer fibres have a strength level of about 1 GPa, where the effect of diameter on fibre strength has almost levelled off according to Fig. 11. The course of the curve in Fig. 11 suggests a Griffith like dependence between strength and fibre diameter, i.e. a linear relationship between strength and the square root of diameter. Strictly speaking the Griffith law relates the strength to crack length, instead of fibre diameter. However, as already pointed out in Section 2, the Griffith equation must be revised if it is applied to common materials, which generally occurs by inserting a factor Y in the equation, which corrects for the geometrical dependence of the strength. This factor Y, in Equation 2, seems however not to be exactly known for the specific case of a surface crack in a cylindrical specimen [26]. The data of Fig. 11 suggest, however, Y to be of the form [20, 61].

$$Y = a(D/c)^{1/2} \tag{7}$$

where a is a constant, D is fibre diameter and c is the crack length. Therefore the strength data were replotted assuming a Griffith type relation of the form:

$$\sigma_b^{-1} = K(D - D_0)^{1/2} + \sigma_0^{-1} \tag{8}$$

In this equation, σ_b is the measured tensile strength. D_0 is the diameter of a flawless fibre, which can be taken zero, since it is about a single chain diameter [61], and σ_0 is the strength of a flawless fibre. K is a constant, which may be of the type, analogous to Equation 2,

$$K = a(1/G_{IC}E)^{1/2} \tag{9}$$

where E is the modulus, G_{IC} the energy needed for the creation of a crack of critical dimensions, and a is a constant relating crack length to fibre diameter and which is an unknown quantity.

Fig. 12 shows that indeed a straight line is obtained if the values of σ_b^{-1} are plotted against $D^{1/2}$. Furthermore a very interesting result is obtained if the line in Fig. 12 is extrapolated to $D = 0$, which yields a flawless fibre strength σ_0 of 26 GPa. This is practically the same as the value for the theoretical strength in polyethylene of

about 25 GPa [10], as estimated from Morse potential calculations on the C–C bond strength in polyethylene. At first sight this result seems purely fortuitous, since the theoretical strength is based on a parallel array of infinitely long extended chains, whereas in the UHMWPE fibres it was found that the strength was determined by topological defect regions in the fibrillar structure and by surface imperfections, i.e. kink bands. However, it could very well be that if the fibres grow thinner, that not only the number of kink bands on the surface is reduced, but that the fibres also adopt a more continuous crystalline structure, i.e. an increasing length of the crystallites. Accordingly the strength would be more and more determined by the covalent bond strength in the molecules instead of the lateral bonding between the molecules. In that case the extrapolation to fibre diameter zero would indeed result in a strength value similar to the theoretical strength in polyethylene. Future investigations are necessary to clarify this point further.

In conclusion we have found that although extremely high molecular weight polyethylene was used in the preparation of the fibres, their practical strength is still mainly determined by the lateral bonding between the molecules. If one wants to approach the theoretical strength of polyethylene it is apparently necessary to prepare extremely thin filaments.

Acknowledgement

This study was supported by the Netherlands Foundation for Chemical Research (SON) with financial aid from the Netherlands Organization for the advancement of Pure Research (ZWO).

The authors wish to express their gratitude to B. A. Klazema and A. T. Doornkamp for their assistance in the SEM experiments and to Drs J. de Boer and H. J. van den Berg for the preparation of the cross-linked filaments. We are very much indebted to Professor Dr A. Peterlin and Professor Dr P. Th. v. Duynen for their valuable comments.

References

1. M. G. NORTHOLT, *Polymer* **21** (1980) 1199.
2. J. R. SCHAEFGEN, T. I. BAIR, J. W. BALLOU, S. L. KWOLEK, P. W. MORGAN, M. PANAR and J. ZIMMERMAN, "Ultra-High Modulus Polymers", edited by A. Cifferi and I. M. Ward (Applied Science Publishers, London, 1979) p. 77.
3. L. S. SINGER, "Ultra-High Modulus Polymers", edited by A. Cifferri and I. M. Ward, (Applied Science Publishers, London, 1979) p. 251.
4. A. ZWIJNENBURG and A. J. PENNINGS, *J. Polym. Sci. Polym. Lett.* **14** (1976) 339.
5. J. C. M. TORFS, J. SMOOK and A. J. PENNINGS, *J. Appl. Polym. Sci.* **28** (1983) 57.
6. B. KALB and A. J. PENNINGS, *J. Mater. Sci.* **15** (1980) 2584.
7. J. SMOOK and A. J. PENNINGS, *J. Appl. Polym. Sci.* **27** (1982) 2209.
8. *Idem*, *J. Mater. Sci.* **19** (1984) 31.
9. A. A. GRIFFITH, *Phil. Trans. Roy. Soc. London* **221** (1921) 163.
10. H. F. MARK, "Polymer Science and Materials", edited by A. V. Tobolsky and H. F. Mark, (Wiley-Interscience, New York, 1971) p. 236.
11. K. E. PEREPELKIN, *Angew. Makromol. Chem.* **22** (1972) 181.
12. A. KELLY, "Strong Solids" (Clarendon Press, Oxford, 1966) p. 7.
13. D. S. BOUDREAUX, *J. Polym. Sci. Polym. Phys. Ed.* **11** (1973) 1285.
14. B. CRIST, M. A. RATNER, A. J. BROWER and J. R. SABIN, *J. Appl. Phys.* **50** (1979) 6047.
15. P. Th. v. DUYNEN, private communication (1983).
16. G. R. IRWIN, *J. Appl. Mech.* **24** (1957) 361.
17. E. OROWAN, Proceedings of the Symposium on Fatigue and Fracture of Metals (J. Wiley and Sons, New York, 1950) p. 139.
18. J. G. WILLIAMS, *Adv. Polym. Sci.* **27** (1978) 67.
19. W. F. BROWN and J. E. STRAWLEY, ASTM STP 410 (American Society for Testing and Materials, Philadelphia, 1966).
20. H. F. BUECKNER, ASTM STP 381 (American Society for Testing and Materials, Philadelphia, 1965) p. 82.
21. A. V. TOBOLSKY and H. EYRING, *J. Chem. Phys.* **11** (1943) 125.
22. S. N. ZHURKOV, *Int. J. Fract. Mech.* **1** (1965) 311.
23. S. N. ZHURKOV and V. E. KORSUKOV, *J. Polym. Sci. Polym. Phys. Ed.* **12** (1974) 385.
24. D. N. BACKMAN and K. L. DE VRIES, *J. Polym. Sci.* **A17** (1969) 2125.
25. S. N. ZHURKOV, V. A. ZAKREVSKYI and V. E. KUKSENKO, *ibid.* **A2 10** (1972) 1509.
26. G. E. R. LAMB, *J. Polym. Sci. Polym. Phys. Ed.* **20** (1982) 297.
27. A. PETERLIN, *Fracture* **1** (1977) 471.
28. D. CAMPBELL and A. PETERLIN, *J. Polym. Sci.* **B6** (1968) 481.
29. A. PETERLIN, *J. Macromol. Sci.* **B7** (1973) 705.
30. E. H. ANDREWS, *Adv. Polym. Sci.* **27** (1978) 1.
31. G. E. R. LAMB and H. D. WEIGMAN, *Text. Res. J.* **47** (1977) 66.
32. D. C. PREVORSEK and W. J. LYONS, *J. Appl. Phys.* **35** (1964) 3152.
33. D. C. PREVORSEK, *J. Polym. Sci. Symp.* **32** (1971) 343.
34. M. G. DOBB, D. J. JOHNSON, A. MAJEED and B. P. SAVAILLE, *Polymer* **20** (1979) 1284.
35. B. D. COLEMAN, *J. Polym. Sci.* **20** (1956) 447.
36. B. D. COLEMAN and A. G. KNOX, *Text. Res. J.* **27** (1957) 393.

37. A. S. KRAUSZ and H. EYRING, "Deformation Kinetics" (J. Wiley and Sons, New York, 1975) p. 331.
38. H. H. KAUSCH, "Polymer Fracture" (Springer Verlag, Heidelberg, 1980).
39. J. de BOER, H. J. VAN DEN BERG and A. J. PENNINGS, *Polymer* in press.
40. J. SMOOK, J. C. M. TORFS and A. J. PENNINGS, *Makromol. Chem.* **182** (1981) 3351.
41. J. C. M. TORFS, PhD thesis, State University of Groningen, Groningen, The Netherlands (1983).
42. J. SMOOK, P. ALFERINK and A. J. PENNINGS, unpublished results.
43. K. TASHIRO, M. KOBAYASHI and H. TADOKORO, *Macromolecules* **11** (1978) 914.
44. A. POSTHUMA DE BOER and A. J. PENNINGS, *J. Polym. Sci. Polym. Phys. Ed.* **14** (1976) 187.
45. D. J. JOHNSON, *Phil. Trans. Roy. Soc. London* **A294** (1980) 443.
46. A. J. PENNINGS and Z. ZWIJNENBURG, *J. Polym. Sci. Polym. Phys. Ed.* **17** (1979) 1011.
47. A. PETERLIN, *J. Macromol. Sci. Phys.* **B19** (1981) 409.
48. P. F. VAN HUTTEN and A. J. PENNINGS, to be published.
49. B. WUNDERLICH, "Macromolecular Physics", Vol. 2, (Academic Press, New York, 1973) p. 392.
50. D. H. RENEKER, *J. Polym. Sci.* **59** (1962) S39.
51. J. SMOOK and A. J. PENNINGS, to be published.
52. S. K. BHATEJA, *J. Macromol. Sci. Phys.* **B22** (1983) 159.
53. J. A. STAMHUIS, PhD thesis, State University of Groningen, Groningen, The Netherlands (1979).
54. D. T. TURNER, *Polymer* **23** (1982) 626.
55. P. PRENTICE, *ibid.* **24** (1983) 344.
56. T. PAKULA and E. W. FISCHER, *J. Polym. Sci. Polym. Phys. Ed.* **19** (1981) 1705.
57. L. JARECKI and D. J. MEIER, *J. Polym. Sci. Polym. Phys. Ed.* **17** (1979) 1611.
58. V. A. MARICHIN, L. P. MJASNIKOVA and Z. PELZBAUER, *J. Macromol. Sci. Phys.* **B22** (1983) 111.
59. D. N. BATCHELDER, C. GALIOTIS, R. T. READ and R. J. YOUNG, Proceedings of the Conference on Deformation, Yield and Fracture of Polymers, Cambridge (1982) p. 21.
60. V. M. NADKARNI and J. M. SCHULTZ, *J. Polym. Sci. Phys. Ed.* **15** (1979) 2151.
61. J. FRIEDEL, "High Strength Materials", edited by V. F. Zackay (J. Wiley and Sons, New York, 1965) p. 1.

Received 6 July
and accepted 28 July 1983